Biomaterials Science

Layer-by-Layer Assembly Methods and Their Biomedical Applications

Journal:	*Biomaterials Science*
Manuscript ID	BM-REV-04-2022-000497.R1
Article Type:	Review Article
Date Submitted by the Author:	04-Jun-2022

Complete List of Authors:	Zhang, Zhuying; Osaka University, Department of Applied Chemistry, Graduate School of Engineering Zeng, Jinfeng; Osaka University, Graduate School of Engineering, Department of Applied Chemistry Groll, Jürgen; University of Würzburg, Department and Chair for Functional Materials in Medicine and Dentistry Matsusaki, Michiya; Osaka University, Graduate School of Engineering, Department of Applied Chemistry

Note: The following files were submitted by the author for peer review, but cannot be converted to PDF. You must view these files (e.g. movies) online.

Revised_manuscript1.docx

REVIEW

Layer-by-Layer Assembly Methods and Their Biomedical Applications

Received 00th January 20xx,
Accepted 00th January 20xx

DOI: 10.1039/x0xx00000x

Zhuying Zhang,[a] Jinfeng Zeng,[a,b] Jürgen Groll[c] and Michiya Matsusaki*[a, d]

Layer-by-layer (LbL) assembly has attracted much interest because of its ability to provide nanoscale control over film characteristics and because of a wide choice of available materials. The methods of LbL not only determine the process properties, but also directly affect film properties. In this review, we will discuss LbL methodologies that have been used in biomedical fields. Special attention is devoted to different properties arising from methods that allow for diverse biomedical applications, ranging from surface modification to tissue engineering. We conclude with a discussion of the current challenges and future perspectives.

1. Introduction

Layer-by-layer (LbL) assembly is a popular and attractive technique to functionalize the surface of a biomaterial and engineer various objects such as capsules and films in a simple, controllable manner. Generally, LbL assembly involves the cyclical deposition of different materials onto substrates, leading to the gradual growth of thin films. The main advantage of this technique is the ability to create stable deposited nanoscale thin films with well-organized structures and tunable composition on different substrates.[1–3] This technology can be traced back to the 1960s when Iler[4] and Kirkland[5] fabricated inorganic films by assembling positively-charged alumina fibers and negatively-charged silica particles. However, it was not until 1997 that Decher,[6] a pioneer researcher, fabricated multilayer films by consecutive adsorption of polyanions and polycations, a more versatile technique that relies on solutions of macromolecules and could thus be successfully extended to other materials. The LbL assembly technique has since experienced a period of explosive growth, being widely used as a versatile, simple, convenient strategy to fabricate multilayer materials with tunable structures, composition, and physicochemical properties.

Many years of development in both the driving forces and assembly methods have seen the current research field of LbL greatly exceed that of Decher's era. The driving forces mostly related to the materials used, the choice of which are highly dependent on their intrinsic properties for desired functions. As well as polyelectrolytes, other materials like synthetic polymers,[7] proteins,[8] nucleic acids,[9] and nanoparticles[10] are also used as building blocks, provided they can interact with each other. The diversity of materials has enriched the interactions of multilayers. Hydrogen bond, host-guest interaction, hydrophobic interaction, and covalent bond are frequently used to drive LbL assembly. Polyelectrolyte LbL assembly films based on electrostatic interactions are still the most commonly investigated as they allow for the quick construction of materials with multiple functionalities, but suffer poor stability once exposed to external stimuli.[11,12] The other aforementioned interactions not only improve the stability and mechanical strength of multilayers, but also provide opportunities to introduce additional functionalities.

Assembly technologies can currently be classified into five main categories: 1) dip assembly, 2) spin-assisted assembly, 3) spray assembly, 4) microfluidic systems and 5) 3D printing. Of these five major assembly technologies, dipping assembly has been researched the longest, while microfluidic systems and 3D printing have been developed more recently. The different LbL methods show unique characteristics, affecting the properties of LbL films such as thickness, surface properties, homogeneity, and internal structure. The advantages and disadvantages of these LbL methods are listed in Table 1.

LbL assembly methods can introduce other forces that help polymer chain rearrangement, directly affecting the physicochemical properties of the film. Spin and spray LbL are forced deposition methods. Their shortened liquid-film contact time combined with high shear force favor stratification in assembly, leaving the adsorbed components as hierarchical multilayers away from conformational equilibrium.[13] Microfluidic systems and 3D printing technologies are high throughput methods with high assembly speed and low material waste. It should be noted that unlike LbL assembly through the dip, spin, spray, and microfluidic systems that are driven by molecular interactions, while LbL via 3D printing is

[a] Department of Applied Chemistry, Graduate School of Engineering, Osaka University, 2-1 Yamadaoka, Suita, Osaka 565-0871, Japan.
[b] Research Fellow of Japan Society for the Promotion of Science, Kojimachi Business Center Building, 5-3-1 Kojimachi, Chiyoda-ku, Tokyo 102-0083, Japan.
[c] Department of Functional Materials in Medicine and Dentistry at the Institute of Functional Materials and Biofabrication (IFB) and Bavarian Polymer Institute (BPI), University of Würzburg, Pleicherwall 2, 97070 Würzburg, Germany
[d] Joint Research Laboratory (TOPPAN) for Advanced Cell Regulatory Chemistry, Graduate School of Engineering, Osaka University, 2-1 Yamadaoka, Suita, Osaka 565-0871, Japan
* E-mail: m-matsus@chem.eng.osaka-u.ac.jp

Table 1 Characteristic of various LbL assembly methods

Methods	Advantages	Disadvantages	General properties	Refs
Dip	Versatile, Shape-independent.	Time-consuming, Low utilization of materials	Become rougher with time.	2, 3, 14, 15, 16
Spin	Rapid, Enhanced mechanical properties.	Only for planar substrate,	Thin and uniform, Low surface roughness Consistent properties across all the bilayers.	17, 18, 19, 20
Spray	Rapid, Shape-independent, Scalable.	Drainage waste of materials	Form multilayers with extremely short contact time, Skip rinsing step, Thinner film, linear growth of film.	21, 22, 23, 24
Microfluidic	High throughput, Low material demand, Patterning.	Device-needed	Patterned films, Microchannel surface modifications.	25, 26, 27
3D printing	High throughput. Low material demand, Rapid and accurate, Fully automated, Patterning.	Expensive, Device-needed	Thicker, Layer wise macroscopic deposition.	28, 29, 30, 31, 32

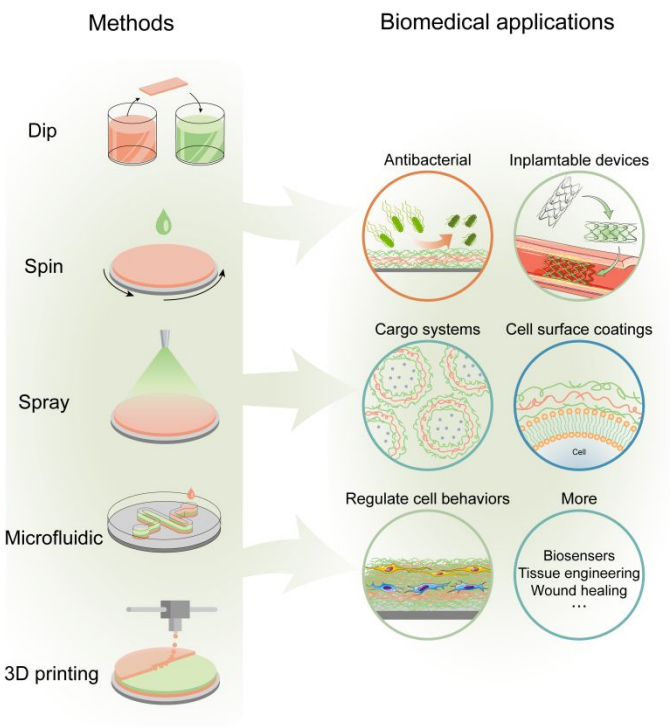

Fig 1 Schematic illustration of different LbL assembly methods and various biomedical applications.

more of a fabrication-driven method that enables macroscopic deposition, that the reason why 3D printed LbL film is always thicker than films fabricated by other methods.

There are already numerous reviews of LbL focused on the interactions,[33,34] fabrication methods,[16,35] and applications.[36–38] These reviews provided us with dense information about LbL from many different viewpoints. Benefiting from the mild conditions and wide range of materials and methods available, biomedical applications such as implant surface modification,[39] cargo systems,[40] and tissue engineering[41,42] have been developed. To mimic biological composition, structures, and functions, specific biomaterials like ligands,[40] proteins,[3] and even cells[43] are used as the LbL components. There are many combinations of materials and methods when fabricating LbL assembly films. Each combination may result in different film properties that are the potential to be applied in suitable circumstances. With all those possibilities, it is vital to settle down a feasible and proper research proposal. The intrinsic chemical properties of raw materials are one of the parameters to predict the fabricated film properties. Some biomaterials are universally used in many biomedical applications like most polysaccharides, but some of them are specific for certain biomedical applications like cells. So as the selection of assembly methods, the appropriate choice of assembly method greatly influences film properties, resulting in materials with specific applications in particular fields. However, it is the processing properties such as versatility, time and labor-saving, and high throughput, rather than the film properties, that are the main reasons why a method is used.

In this review, we will particularly focus on the process properties of different LbL assembly methods and film properties and applications originating from each method (**Fig 1**) for the first time. By reviewing the LbL assembly methods, film properties, and potential biomedical applications, we can glimpse the ingenuity and subtlety of the LbL assembly technique. To convey the relationship between the process parameters that straightforwardly affect the film properties, we summarized the relative information in Table 2. We hope this review would act as a guide for assembly method selection on film fabrication for biomedical applications.

Table 2 Summary of key process parameters that affect the film properties reported in the representative studies and their performances in biomedical applications.

Methods	Process parameters	Properties	Performances	Applications	Refs
Dip	Dip time	Molecule interdiffusion	Pore volume fractions	Drug delivery	44
	Rinsing time	Interdigitation	Stiffness	Cell adhesion regulation	45
Spin	Spin speed	Thickness and roughness	Triggered release rate	Antibacterial coatings, antibiotic delivery	46,
		Thickness and molecule conformation	pH-stability		13
		Thickness	Adhesion strength	Sealing effect	47, 48
	Contact time	Molecule conformation	pH-annealing/pH responsive,	Controlled drug releasing	13
		polar interactions	Adhesion forces	Cell-attachment regulation	49
Spray	Spray flow rate	thickness			50
		Surface morphology	Functionalize porous material or bridge the network		51
	Spray duration	Thickness			52
		Surface morphology			52
		Assembly time	Bridging the porous substrate	Mimic skin structure, surface coating	53, 54
	Droplet size	Surface morphology, roughness			55
	Simultaneous spray or not	Uniformity			52
		Film interdiffusion	Drug-loading amount	Drug delivery, drug release coating	56, 57
		Nanoparticle organization	The nanometer-scale precise distribution of NPs	Tailorable delivery timescale	58
Microfluidic system	Contact time	Thickness	Tube diameter		59
		Equilibrium/nonequilibrium state			60
	Chamber shape	Patterned functionalized surface	Micropatterned cell co-cultures		61, 62, 63
		LbL dynamic pattern		Tissue engineering	25, 64
		Micro channel surface modification	Biocompatibility, mechanical properties	Enzyme immobilization, cancel cell isolation	65, 66
			Surface coatings on micro devices	Bio detection	67
3D printing	Droplet size (resolution)		Cell density	Tissue printing	28
	Printing in support bath			Tissue engineering	29
	Patterned printing			Tissue engineering	68
	Laser-assisted bioprinting		Cell-density	Tissue engineering	69

2. Dip assembly

Dip assembly is the most common LbL assembly method, involving the alternate adsorption of two or more different desired material solutions, with intermediate washing steps.[70,71] It is usually performed by manually immersing a substrate into a solution of the desired materials to modify the surface function.

The film properties are influenced by solution properties such as concentration and charge density, as well as process parameters such as dip time and rinse time.[20] Specifically, a higher concentration increases the quantity of adsorbed materials, leading to a thicker nanofilm. High concentration can also increase the viscosity of the solution, slowing the rate of material diffusion and prolonging the time for the films to reach equilibrium. It should be noted that when solution concentration is below a certain level, interdigitation between the layers occurs as a result of interdiffusion. However, cell adhesion is enhanced on the interdigitation layers as the result of increased stiffness.[45] The dipping time for the adsorption of each layer is of crucial importance. A short dipping time results in kinetically trapped polymers,[72] while a longer dipping time allows for adequate layer deposition and polymer chain rearrangement. However, a much longer dipping time can weaken the stratified structures of the films.[14] Dip LbL assembly on different substrates[15] has a variety of potential biomedical applications.

2.1. Planar substrates

LbL assembly on planar substrates is the most widely used and most important method of dip assembly. It has been applied in

several biomedical fields like the modification of substrates to improve the biocompatibility or to add specialized properties by selecting functional materials as their components.

2.1.1. Regulation of cell behavior

Cell behavior on LbL assembly films can be regulated by stiffness, morphology, biological properties, and release properties of films.[73] The chemical properties of multilayers are highly dependent on their composition. For example, cell adhesion is promoted by the use of materials that are known to have adhesive properties. Arginine-glycine-aspartic acid (RGD) [74–76] and catechol groups,[77,78] either acting as an assembly component or as a partial structure of the polymers, have been used to support cell and protein adhesion due to the enriched interactions between surfaces and cells.

For the control of other cell behaviors like proliferation and differentiation, more complex structures and accurate adjustment of surface properties are required. Chitosan/fibrinogen multilayers have been fabricated for improving the adhesion and spreading of cardiomyocytes.[79] It was reported that a pure fibrinogen coating was sufficient for cell adhesion and spreading, but chitosan tuned the absorbed fibrinogen amount, facilitating the identification of the optimal surface properties for cell proliferation. Another method for constructing cell regulation LbL films is using LbL film as a delivery reservoir for bioactive molecules. Pichart's group[80] has loaded bone morphogenetic protein 2 (BMP-2) into poly(L-lysine)/hyaluronan (PLL/HA) films. The post-loaded BMP-2 were protected by LbL film and delivered to cells, inducing myoblasts to differentiate into osteoblasts.

Controlling protein adsorption and cell adhesion is important for a wide range of biomedical applications. It is known that the final layer's surface charge and hydrophobicity of the materials govern protein adsorption and cell adhesion. To provide a set of guiding principles for making films that promote cell and protein adhesion, a new model based on LbL with independent control over the surface charge and hydrophobicity was developed.[81] Substrates coated with serial multilayers with a surface isoelectric point (p*I*) in the range of 5-9 and water contact angle (CA) of 35-70° were used to test their cell adhesion (**Fig 2**). The results revealed that a positive charge and hydrophilicity lead to high cell adhesion, whereas a negative charge and hydrophobicity lead to low cell adhesion.

2.1.2. Controlled drug-releasing properties

The releasing properties of a film are usually achieved by stimuli-responsive residues. For LbL films, electrostatic interactions, hydrogen bonds, and host-guest interactions are generally non-covalent interactions and a drastic change in the external environment, such as pH and temperature, will result in the dissociation of multilayer films in an aqueous solution. This dissociation can be exploited to create responsive burst release systems.[82]

When two or more types of interactions are induced, it is possible to break just one kind of interaction and retain the other. Based on this, a reusable platform for protein and bacterial capture and release was developed.[83] The platform was assembled via host-guest interactions and electrostatic interactions. Because of the inherent reversibility of host-guest

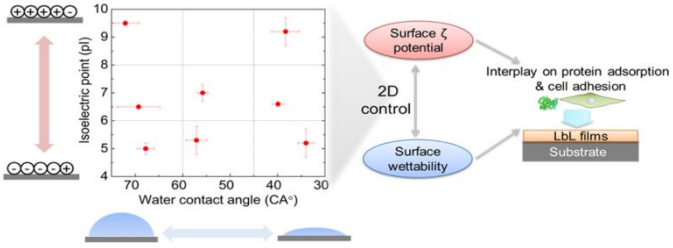

Fig 2 Schematic diagram showing the rationale for the surface designs developed in this work. Reproduced with permission from ref. 81. Copyright 2016 American Chemical Society.

interactions, the paired structure was dissociated by incubating with sodium dodecyl sulfate without destroying the structure of the multilayered film, allowing the captured proteins and bacteria to be released from the platform and then renewing the "guest" surface for the next capture of proteins and bacteria.

To improve the stability of the assembled film for wider application, the electrostatic interaction and hydrogen bond can be further crosslinked to form covalent bonds in physiological conditions. Different crosslinking methods (photo crosslinking,[84] thermal crosslinking[85]) can be chosen based on the chemical properties of film components. After partial crosslinking, there are both stable and reversible interactions that enable the film to respond to stimuli while maintaining the LbL structure, allowing for controlled release.[86]

2.2. Medical devices substrates

Dip assembly shows a non-shape-limited property, making it ideal for the surface modification of irregular-shaped implanted devices. The layer-by-layer coating on medical devices adds functionality relevant to specific applications, making them more suitable for regulating cellular behavior and for tissue engineering. To prevent in-stent restenosis after surgery, cardiovascular stents have been coated by chitosan/heparin multilayers with embedded epigallocatechin gallate/copper (EGCG/Cu) complexes to mimic the basic function of endothelial cells, thus enabling rapid in situ endothelialization and suppressing smooth muscle cell proliferation.[87] Similarly, to prevent fatal thrombosis and intimal hyperplasia, an artificial vascular graft based on polycaprolactone has been produced with LbL coatings for long-term antithrombogenicity and anti-inflammatory properties.[88] In the case of bone regeneration implants, efforts have been made to enhance their biological performance, which often entails physical, chemical, and biological modifications to the implants. Bio functional peptides are induced to guide the differentiation of bone marrow mesenchymal stem cells into osteoblasts.[89] Collagen/chondroitin sulfate multilayers have been assembled onto the surface of an implant and used as a precursor matrix to promote mineralization, thereby encouraging osteogenic differentiation of MC3T3-E1 cells.[3] To help prevent implant-associated infections, antibacterial coatings have been constructed on the surface of implants. One study used hydroxypropyl trimethyl ammonium chloride chitosan (HACC), with release-killing and contact-killing functions, as the antibacterial reagent.[39] By selecting an appropriate degree of

quaternary ammonium substitution, HACC can strike a balance between antibacterial efficacy and cytocompatibility. The interesting thing is before constructing functional film on implantable devices, pre-studies of the film properties on planar substrates is conducted. For example, as we mentioned in 2.2.1, Pichart's group first studied the LbL film's osteoinductive ability on planar substrates,[80] then conducted the assembly process on titanium implants[90–92] and poly(etheretherketone) PEEK implants[91] to improve their bone regeneration abilities. Thus, by altering the surface properties of implantable devices, it is possible to manipulate cell behaviors or protein expressions to mimic cell functions for enhanced features.

2.3. Microparticle substrates

Dip assembly can be performed on micro- and nanoparticle substrates. Compared with macroscopic substrates, they are too small to be filtrated and precipitated, requiring extra separation steps between deposition and washing, which are typically conducted via centrifugation.[93] After assembly is finished, hollow capsules are obtained by removing the substrates without disrupting the multilayers.[94]

2.3.1. Microcapsules

The dip assembly technique on nanoparticles has been driven by the need of drug delivery to effectively encapsulate, protect, and deliver bioactive substances. Similar to assembly on planar substrates, the driving force and interactions between the LbL assemblies on nanoparticles have an impact on their releasing properties (as mentioned in 2.1.2 Controlled drug releasing properties).

Other functional groups can be introduced to the microcapsules to allow triggering methods such as UV [95] and redox-triggering, and response to biological stimuli (enzymatic cleavage).[96] However, these LbL microcapsules can only release the loaded drug by an irreversible deteriorative self-disassembly mode. By introducing two types of functional groups, one stable and the other stimuli-responsive, the microcapsules can be both structurally stable and responsive,[97] making them applicable for re-usable drug release.

The microcapsules themselves can serve as substrates to support a new LbL assembly on the surfaces. Mano and his co-workers fabricated compartmentalized capsules, where microcapsules are embedded in macroscopic beads coated with a LbL shell.[98,99] Such co-capsules can act as transportations and reservoirs for bioactive agents and cells in tissue engineering applications.

2.3.2. Cell encapsulation

Encapsulating living cells has garnered considerable interest in biomedical fields, like transplantation therapy, tissue engineering, and cell-based biosensors. Numerous reviews have focused on the materials,[100] strategies,[101,102] and applications,[103–105] of cell encapsulation. Briefly, a variety of materials have been used for LbL cell encapsulation including polysaccharides, proteins, and even nanoparticles.[106,107] Living cells are more sensitive to their surroundings so the encapsulation process must be performed under physiological conditions to maintain cell viability.[108]

Cell encapsulation enables attenuation of the host immunological response in cell transplantation,[109] incorporation of functional molecules to regulate cell biological behavior, and modification of the cells' surface to endow them with new features for tissue engineering,[110] etc. Our group has successfully constructed extracellular matrix (ECM)-like films on a cell surface with the layer-by-layer assembly of fibronectin (FN) and gelatin (G). The FN/G film acted as an ECM-like support,[111] protecting the cells from contact inhibition and promoting cell-cell adhesions.[112] This technology will be promising for the engineering of 3D tissue.

The substrates can be considered as templates for LbL assembly. The shapes of assembled films are dependent on the shapes of substrates. Except for the discussed planar, medical device, and microparticle substrates. Dip LbL assembly on other shapes could result in films with interesting structures. Like LbL assembly on granular 3D structure, with the help of perfusion technique, this method can fabricate interconnected hollow capsules in 3D space.[113,114] LbL assembly on tube-like substrates followed by leaching the substrates leaving hollow-tube-like films.[115] By designing the substrate shape, it is easy to construct desirable structures with tailorable surface properties, which opens new prospects to create complex 3D constructs for tissue engineering applications.[114]

Dip assembly is the simplest and most widely used LbL method. The properties of films fabricated by this method are mostly related to the material properties. Dip time and rinsing time are the only two process parameters that affect the film's properties. The film stiffness and internal structure can be adjusted to suit cell adhesion and drug loading.

3. Spin-assisted assembly

LbL assembly by spin coating is also known as spin-assisted assembly.[116,117] It is the combination of LbL with the spin-coating method, which is a simple, fast, highly controllable, and reproducible technique for depositing a solution onto a spinning substrate.

Numerous parameters influence the thickness and morphology of spin-assisted assembly films, including spin speed, solution concentration and viscosity, and evaporation rate.[118,119] Spin speed is a critical factor that affects the centrifugal force and evaporation rate. Thinner films are generated at a higher spin speed[46] and the concentration of the solution also has an effect on film thickness. It has been commonly observed that the film thickness increases with the concentration.[49] For non-Newtonian fluids like polymeric solutions, higher concentrations generally result in increased viscosities, which contribute to thicker films by restricting fluid flow. During the coating process, solvent evaporation alters the physical properties of the solution, affecting the uniformity of the film thickness. During the spinning process, the angular velocity increases with increasing distance from the substrate center, resulting in changes in the fluid viscosity as it dries toward the edge, which may cause nonuniform radial thickness. A slower evaporation rate helps to maintain a more constant viscosity across the substrate, improving the uniformity of

thickness. In general, a slower spin speed, higher viscosity, and a slower evaporation rate result in a thicker and more uniform layer.[120] Furthermore, temperature, airflow velocity, and humidity also have a great effect on the film. By adjusting the spinning parameters, the morphology and other properties of films can be successfully controlled.

Unlike dip assembly, which is dependent on the diffusion speed of polymer chains, spin assembly is more productive due to centrifugal and shear forces, which promote chain rearrangement on the substrate much more quickly than free polymer diffusion. While the dip assembly step takes a few minutes, spin-assisted assembly takes only a few seconds.[18] In the spin-assisted assembly process, shear forces reduce the quantity of polymer absorbed, resulting in a thinner film with a more ordered internal structure.[46] Centrifugal forces generated during the spin process flatten the polymer chains, leading to slower diffusion parallel to the substrate.[17]

The shorter liquid-film contact period and shear forces produced by spin assembly result in more ordered multilayers but are thought not to be sufficient to relax polymer chains, resulting in non-equilibrium conformation in multilayers.[13] The kinetically trapped polymer chains are hypothesized to relax slowly in multilayers.[121,122] Post-assembly treatments can be used to facilitate such chain rearrangements, resulting in a change in the characteristics before and after treatments. For electrostatic and hydrogen-bond LbL films, treatment methods include salt treatment[123,124] and pH treatment.[44,125] Post-treatments have been shown to result in the relaxation and reconstruction of polymer chains into more equilibrated conformations,[124] accompanied by an enhancement of film stability[126] and changes in surface properties.[127] The nonequilibrium state of spin-assisted LbL films is more sensitive to external stimuli before post-treatment but more stable after and this feature is of critical importance in practical applications of electrostatic or hydrogen bond LbL films as a platform for controlled release.

The process of spinning requires a planar substrate, so this method is limited to the preparation of planar films. Following their assembly on planar substrates, films perform their job either on the substrates or detached from the substrates. In the former scenario, films are referred to as functional coatings while in the latter they are referred to as freestanding films.

3.1. Cell controllable films

Due to the effectiveness of spin-assisted LbL assembly, the production of functional coatings is very common and widely used in biomedical applications. Cell adhesion to the substrate is the first step in the production of biomaterials for a variety of applications, including tissue engineering and implantable biomaterials. The physicochemical parameters of the matrix, which include charge density, wettability, stiffness, and roughness, affect the cell adhesion property.

Switching the outermost layer of LbL coatings is one of the simplest ways to alter surface properties,[49] as free functional groups of the outermost layer enable easy post-modification of the surface properties for various potential applications. Liu[128] fabricated polymer multilayered films using sulfur(VI)–fluoride exchange (SuFEx) click reaction via spin-assisted LbL deposition from a sulfonyl fluoride-rich polymer. These films retain the residual sulfonyl fluoride functionality and can be conveniently post functionalized via the SuFEx click reaction to impart antifouling or antibacterial properties. Polymers can be modified to satisfy the requirements for developing multifunctional films for tissue regeneration. The modification of carboxymethyl chitosan and oxidized alginate with RGD and dopamine has been shown to increase cell adhesion and antioxidative properties, prolonging the survival of cells.[129]

Another strategy for regulating cell behavior is the introduction of bioactive compounds into multilayers. For instance, Minocycline (Mino), a well-established antibiotic that acts as a collagenase inhibitor and zinc chelator, can also promote bone growth.[130] Modifying titanium (Ti) substrates with Mino embedded in gelatin/chitosan multilayers promotes osteogenesis.[131] With the sustained release of Mino, Ti substrates effectively regulate the behavior of mesenchymal stem cells (MSCs) and macrophages.

3.2. Freestanding film for tissue engineering

Due to the high-speed horizontal polymeric diffusion that occurs during the spin process, the spin technique produces exceptionally homogeneous films with flat and smooth surfaces that are easily detachable from the substrates. The separation of films from their substrates enables direct characterization of a variety of features,[132] permitting applications in biomedical fields. The self-supporting films can be transferred to any other support used as a scaffold for use in tissue engineering, drug loading and delivery systems, or cell culture platforms.

The manufacture of freestanding films is basically identical to that of conventional functional spin coatings. However, a final detachment step is required, which is also the most challenging, as defects may be introduced or the surface roughness may be altered.[133]

There are several methods for completely detaching the films from the substrate. Some require further processing while others rely on the inherent mechanical characteristics of the materials and surface properties of bare substrates. But the key point when choosing a suitable method of detachment is to avoid interfering with the properties of the films.

For detachment, the film should be of sufficient strength to withstand the force applied when it is peeled away from the substrate. There are reportedly two ways to accomplish this: 1) decrease the interaction between the film and substrate, 2) enhance the mechanical properties of the film.

1) Decrease the interaction between the film and substrate.

The most commonly used method for decreasing or eliminating the attachment force of spin-coated films is to incorporate a sacrificial layer prior to actual film fabrication. After dissolving the sacrificial layer, the films can be suspended in solution.[133] Choosing a suitable solvent can not only dissolve the sacrificial layer, but also break the interaction between the films and the substrate. For example, salt solutions have been used to dismantle electrostatic interactions and hydrogen bonds. Additionally, LbL films have been fabricated on low surface energy substrates, like Teflon,[134] polypropylene,[135] and

polystyrene.[136] Due to the weak van der Waal's interactions between the initial layer and the substrate, films can be easily detached without any post-processing step, which is the most adaptable and straightforward method. Except for polymer films, cell sheets can also be detached from the culture substrate, making use of the hydrophobicity switch of a poly(N-isopropylacrylamide) (PNIPAAM)-based thermo-responsive surface. When the temperature is lowered to the lower critical solution temperature (LCST), the polymer surfaces become hydrophilic, forming a hydration layer between the cultured surface and cells, allowing for their detachment without enzymatic treatment.[137,138]

2) Enhancement of the film's mechanical properties

Another way to obtain freestanding films is to improve their mechanical qualities so that they can be directly peeled from the substrate without a sacrificial layer.[49] This can be achieved by depositing a further supporting film after LbL assembly which confers additional mechanical strength, allowing films to be easily peeled from the substrate.[139–141] After removal from the substrate, the supporting layer also contributes to the stability of the LbL assembled nanostructures.[47,48] As a result, the nanofilm can be transferred and applied to other surfaces together with the supporting layer to avoid fracture.

Because of the versatility and flexibility of LbL assembly, the surface properties of the films can be easily modified before bringing them into contact with cells and tissues. Freestanding films have a wide range of potential biomedical applications.

One novel application is mucosal defect repair,[142] which requires a stable adhesive platform with ultrathin thickness, a smooth surface, and a high aspect ratio. Freestanding films made with spin assembly adequately fulfil these requirements. Ultrathin films adhere strongly to organ surfaces but do not adhere to neighboring organs, reducing the risk of adhesive complications after surgery. Before detachment, like other LbL films, drugs can be loaded into the multilayers, then the therapeutical effect is synergic with the wound healing and drug-releasing properties.

Similar to other LbL assemblies, other therapeutic composites can be embedded into the multilayers. As shown in **Fig 3**, Redolfi Riva[143] sandwiched gold nanoparticles into multilayers of chitosan/alginate and then the film was peeled off after casting a PVA supporting layer. This freestanding film could be used for cancer therapy through thermal tissue ablation. Moreover, the mucoadhesive properties ensure durable attachment to mucosal tissue, allowing for precise distribution and density control of nanoparticles, providing safer photo thermalization compared to conventional laser surgery.

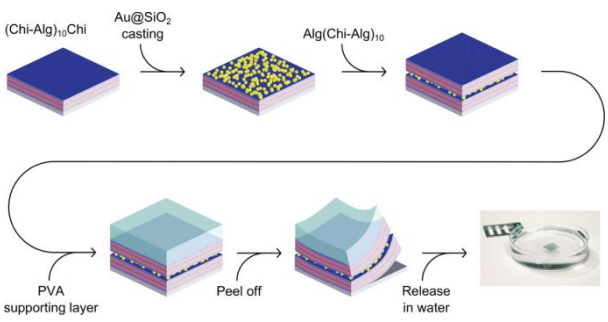

Fig 3 Preparation scheme of free-standing thermonanofilms and snapshot of nanofilm freestanding in water. Reproduced with permission from ref. 143. Copyright 2014 American Chemical Society.

Spin-assisted assembly is a more controllable LbL method compared with dip assembly. Spin speed and contact time are the main two parameters during the process. But more film properties can be affected by these two process parameters, like thickness, surface roughness, and molecule conformation, affecting the loading and releasing properties. Generally, spin-assisted assembly films show better mechanical properties, which expand their application in wound healing.

4. Spray assembly

Spray LbL assembly is another frequently used assembly method, in which films are assembled by aerosolizing polymer solutions or suspensions and sequentially spraying them onto substrates.[144,145] Interestingly, spray assembly does not always need intermediate rinsing steps, as the spray of the subsequent solution will rinse away any polymer that was not bonded to the previous layer. Spray assembly possesses the benefits of both dip and spin assembly. It is adaptable to substrates with varying geometries[24,146] and absorbs a new layer in just a few seconds. The fabrication time of spray assembly LbL films has been greatly shortened due to the enhanced adsorption by the spray pressure.

In spray LbL assembly, the film properties can be tuned to be similar to those of dip assembly. The film thickness is influenced by solution concentration, spray flow rate, spray duration, rinsing duration, and whether or not the layers were dried after spraying.

In contrast to dip LbL assembled films, sprayed LbL films have been found to be substantially thinner.[56] In terms of film homogeneity, spray assembly appears to result in more regular LbL films than dip assembly,[145] even in the absence of washing procedures. This occurs because the newly sprayed polymers quickly and thoroughly mix with the deposited layer, whereas with dip assembly this process takes markedly longer. Compared with spin assembly, spraying is much faster and easier to adapt at a large scale level.[147]

While the majority of spray assembly methods use alternate spraying of two solutions, it has been demonstrated that film can also be formed using simultaneous spraying, in which two solutions are sprayed onto the substrate at the same time.[52] Simultaneous spray assembly is a process that relies on the rapid interaction of two components. It causes the formation of complexes in the solution before reaching the substrate (**Fig 4a**), resulting in the continuous growth of a film. The film thickness increases linearly as the complexes accumulate, i.e., with the spraying time. There is a strong correlation between the size of the complexes and the film growth rate, and this rate is highly dependent on the interacting domain ratios. Because of the film growth mechanism, the resulting film topography is granular, and both the roughness and growth rate of the film are related to the polyanion/polycation ratio.[50]

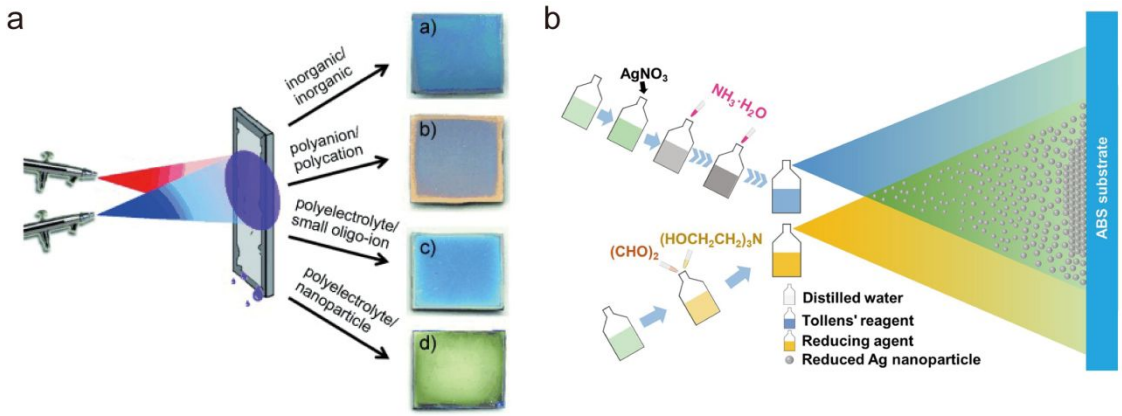

Fig 4 (a) Representation of the simultaneous spray assembly and images of films deposited on silicon wafers: a) NaF and $CaCl_2 \cdot 2H_2O$, b) PAH and PSS, c) PAH and sodium citrate, d) PAH and gold nanoparticles. Reproduced with permission from ref. 52. Copyright 2010 WILEY-VCH. (b) Schematic diagram illustrating the process of preparing solutions and simultaneous spray deposition. Reproduced with permission from ref. 55. Copyright 2019 Elsevier B.V.

The reaction between two solutions does not always refer to the complex of two components as other reactions like metallic reduction may also occur. Chen[55] expanded the simultaneous spraying technology to prepare metallic coatings. As illustrated in **Fig 4b**, Tollen's reagent and a reducing solution were sprayed simultaneously over the substrate and then reacted to form Ag nanoparticles that accumulated as a layer on the substrate.

4.1. Porous substrate

Spray LbL assembly enables rapid coating of structurally complicated and porous substrates, thus improving their functionality. This is especially applicable for rapid hemostasis materials, such as bandages, sponges, and gauzes. The development of a multilayer film made of hemostatic components on gelatin sponges was found to be effective for rapid hemostasis in a pig spleen hemorrhage model.[54]

If the pores on a surface are below a certain size, spray deposition can bridge the pores, coating the surface rather than penetrating the full thickness of the film.[51] Monteiro[53] took advantage of the pore-bridging ability of spray deposition to produce a stable and dense hyaluronic acid (HA)/poly-L-lysins (PLL) coating on top of porous HA membranes, simulating the epidermal and dermal components of skin respectively, and thereby establishing a scaffold for full-thickness skin regeneration (**Fig 5**). Furthermore, the rapidity of spray LbL assembly prevents excessive swelling of the hydrophilic substrate HA membrane during top film assembly, thus preserving the original structure of the substrate. This strategy can be used to mimic other multi-layered ultrathin biostructures.

4.2. Embedding therapeutics in polymer multilayers

Unlike conventional bulk materials, which have a therapeutic loading capacity limit, LbL assembly has demonstrated a high degree of adaptability in terms of embedding and delivering biologically active components. The spray LbL assembly process can be used to increase drug loading and control interdiffusion of a drug, thus enhancing the interaction of film components. It has been shown that spray assembly helps promote the formation of interactions between vancomycin (a potent multispectrum antibiotic) and multilayers, improving the maximum drug loading to approximately 20 wt%, a remarkable figure as typical drug loading rates are limited to just a few weight percent.[56] This strategy provides an insight into how to directly incorporate small and weakly charged molecules in multilayers and has been expanded to more than one kind of drug.[57] Regardless of loading and release efficiency, the optimal therapeutic effect of pharmaceuticals can be obtained by altering the number of bilayers covering the medications.[148]

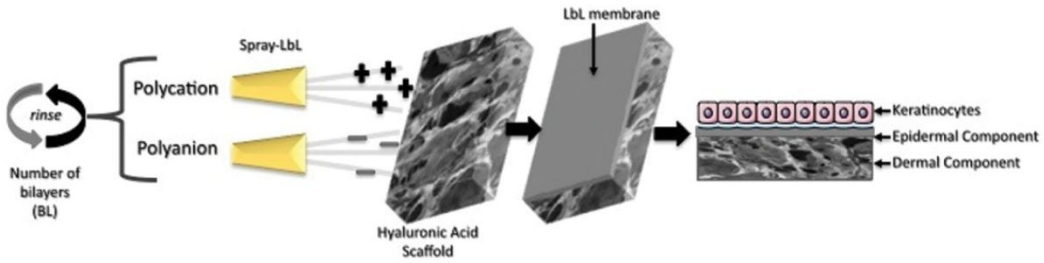

Fig 5 Schematic of the approach. The polycation, poly-L-lysine, and the polyanion, hyaluronic acid, are sprayed on top of the hyaluronic acid porous scaffold, creating a layer-by-layer membrane. Keratinocytes are seeded on top of the membrane, forming a cell monolayer. The layer-by-layer membrane acts as an epidermal substitute, which adheres to the dermal component (the porous hyaluronic acid scaffold).Reproduced with permission from ref. 53. Copyright 2014 WILEY-VCH.

LbL assembly enables precise control of the vertical dispersion of nanoparticles at the nanoscale. However, aggregation of nanoparticles is a frequent occurrence and presents a major obstacle. The spraying pressure may help prevent aggregate formation, resulting in a more controlled distribution of nanoparticles compared to dip assembly.[58]

Spray LbL assembly can be conducted with only nanoparticles. AgNPs loaded with nanotubes have been modified with positively charged chitosan and a negatively charged synthetic heparin-like polymer, then alternately deposited on substrates via spray-assisted LbL assembly. Benefiting from the universal and large-scale fabrication advantage of spraying, Nie[149] produced a self-sterilizing coating with biocompatibility and antibacterial properties. This proposed strategy can be applied to the design of many other kinds of nanoparticle-based coatings.

The thickness of LbL film reflects the accumulated amount of polymer. In spray assembly, that is affected by the spray flow rate and the spray duration. Except for thickness, the surface morphology of the films can be regulated. Not only the films themselves but also affect the substrate's morphology, since the sprayed solution is able to bridge the porous structure.

5. Microfluidic systems

Microfluidic LbL assembly uses fluidic channels to deposit multilayers on both the channel walls[150] and the substrate immobilized in the channel.[67] Microfluidic assembly is normally performed with a pump, where solutions in the perfusion chamber can be driven by vacuum or pressure. Polymer solutions can be pulled into channels by capillary forces, then solutions can be pulled into channels by capillary forces, then rapidly rotated to remove the surplus solution from channels.[151] Capillary assembly is simple and does not require external pumps, but it is not ideal for larger quantities or when a precise flow rate is needed.

It is notable that if polymer solutions remain static in microfluidic devices,[152] the results of fluidic assembly strongly resembles those of dip assembly. Thus, for fluidic assembly, contact time rather than the flow rate is the primary determinant of the adsorbing amount of polymer under flow. As with other methods, the surface roughness and thickness increase as the concentration of solution increases.[60]

5.1. Region-selective patterning

Microfluidic devices with perfusion chambers can be used to achieve region-selective deposition (**Fig 6**). With specially designed microfluidic molds, fluidic assembly can be used to generate functional coatings with complex patterns. Cells and other materials can adhere preferentially to the pattern area, resulting in the formation of three-dimensional cellular structures.[61,62]

Dynamic patterning can be accomplished with the aid of a computer and a digital micromirror device (DMD), which is capable of controlling over one million small mirrors to project a pattern of high-intensity UV light onto the DMD panel.[153] Following this UV exposure, the photosensitive precursor crosslinks and forms a pattern on substrates or the previous layer. The combination of DMD technology with the microfluidic device enables layer-by-layer bioprinting.[25] By introducing cell-laden gelatin methacrylate (GelMA) into the microfluidic device and changing the pattern and concentration of each layer, this strategy can be used to construct a high spatial resolution 3D vascular structure with neovascularization potential. Except for the in situ stacking of different layers, a DMD-based microfluidic system can be used to fabricate different single micromodule layers with center holes, then the micro modules are assembled layer-by-layer via hydrodynamic interactions, forming hollow 3D tissue-like constructs.[64]

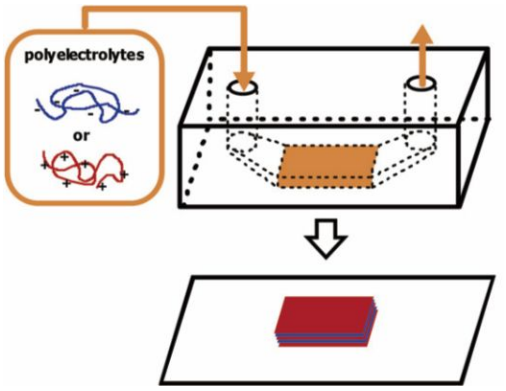

Fig 6 Fluidic device used to deposit polyelectrolytes on limited region of substrates. Reproduced with permission form ref. 26. Copyright 2005 American Chemical Society.

5.2. LbL assembly on cylindrical microchannels

Fluidic assembly is not limited to planar substrates. If the inner surfaces of tubes or capillaries need modifications, microfluidic LbL assembly is a possible method. By infusing solutions into a tube, antifungal assembly films can be used to modify the interior wall of catheter tubes to prevent fouling.[154] Apart from the surface properties change of a single tube, the size-narrowing effect of microchannels can also affect the overall performance.[155] Based on a newly developed all-liquid microfluidic chip, microfluidic LbL assembly was recently used to construct a biocompatible interface on the inner walls of microchannels (**Fig 7**). The multilayer coatings can improve the mechanical properties and provide a biocompatible environment for enzyme immobilization.[65] The coatings in a microfluidic chip can also serve as biosensors, detecting cancer cells[66] or particular proteins[156] depending on their specific interactions.

The microfluidic channels themselves can serve as a template to fabricate tubular-like structures. 3D scaffolds with microchannels in the order of tens of micrometers were first functionalized with hyaluronic acid/chitosan LbL films grafted with RGD, then human umbilical vein endothelial cells (HUVECs) were seeded on the coatings, mimicking a vascular capillary structure.[157] The outside of the channels can be modified with a specifically designed microfluidic device. As shown in **Fig 8** chondroitin sulfate (CS)/chitosan (CHI) hollow fibers were

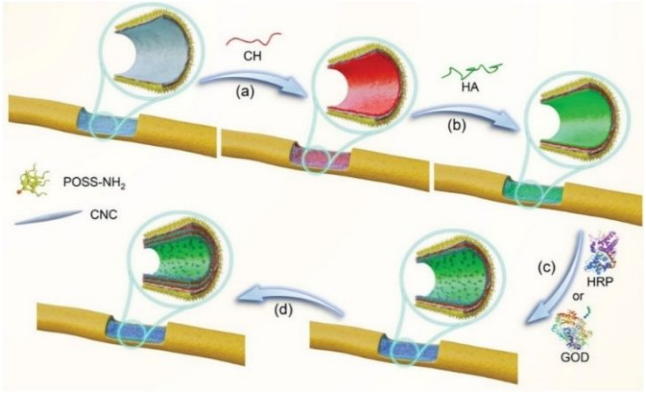

Fig 7 Schematics showing the layer-by-layer (LbL) assembly process of chitosan (CH) and hyaluronic acid (HA) for enzyme immobilization in an all-liquid microfluidic chip. a, b) The sequential deposition of CH and HA on the inner wall of the microchannel. c) The immobilization of horseradish peroxidase (HRP) or glucose oxidase (GOD) on the CH/HA multilayer. d) Repeated procedures of (a-c). Reproduced with permission from ref. 65. Copyright 2021 WILEY-VCH.

fabricated using a microfluidic device and connected with epoxy resin microchannels. Endothelial-loaded core flow and fibroblast-loaded sheath flow merged with hollow fibers and coated the inside and outside of fibers respectively, forming a blood-vessel-like structure.[158]

5.3. Microparticles and Capsules

Using the homogeneous particle size distribution and very accurate interfacial contact interaction,[159] microfluidic assembly can be used to coat tiny particles, including fragile cells, with functional components.[160] Neuronal cells can be patterned with a pre-designed fluidic device.[63] Microfluidic assembly can encapsulate cells by putting them into fluidic channels, then using vacuum or pressure to sequentially flow polymers and wash solutions through them. Both cell islets and single cells can be coated for protection, allowing for in vivo transplantation.

Microfluidic technology can also be used to generate LbL microcapsules with separate layer cavities. A unique gas-liquid microfluidic device has been developed to introduce cavities.[161] As shown in **Fig 9a**, a solution of carboxymethyl cellulose (CMC, negative charge) was introduced into a microfluidic device via a syringe pump and subsequently sheared into small droplets using N_2 at the nozzle of the capillary. The small droplets landed in the chitosan (CS, positive charge) solution, forming single bilayer capsules. The CS solutions containing single-bilayer capsules were injected into a second device with a larger diameter, and the assembly procedure was repeated to generate microcapsules with two CMC/CS bilayers. This is a simple and effective method for fabricating LbL microcapsules with cavities between each bilayer. Drugs, bioactives, or nanoparticles can be enclosed in the voids of each layer, allowing for a novel type of cargo delivery system design.

In summary, fluidic assembly enables the construction of multilayers on surfaces that are inaccessible by conventional methods, like assembly inside capillaries or tubes. It also introduces a novel method for region-specific patterning through the use of fluidic devices. It is a valuable tool for coating sensitive particulate substrates, like cells, that may be damaged in centrifugation-based separation. These unique advantages make it an attractive option for many biomedical applications, even when specialized equipment such as fluidic devices and pumps are required.

In some ways, a microfluidic system can be considered as a mini dip assembly method. So the thickness of the films is mostly affected by contact time. The different thing is the shape of the chamber and microchannel sometimes serve as LbL assembly templates, restrict the assembly area and form patterned films. LbL in microchannels and precise control of assembly region make microfluidic systems popular in tissue engineering.

6. 3D Printing

3D printing, which evolved from 2D printing and has since revolutionized numerous areas in biomedical fields, is an additive manufacturing method. In biomedical applications, 3D printing facilitates the construction of complex biomimetic structures with biocompatible materials,[162] bioactives, and living cells.[163] Moreover, the layer-by-layer precise spatial control over deposition enables it to be applied to tissue engineering,[164] such as for the creation of transplantable tissues.[29,165] When printing biologically sensitive materials and living cells, an important issue is maintaining their activity. This section will review the 3D printing strategies for biomedical applications (bioprinting) and discuss the shortcomings of current methods.

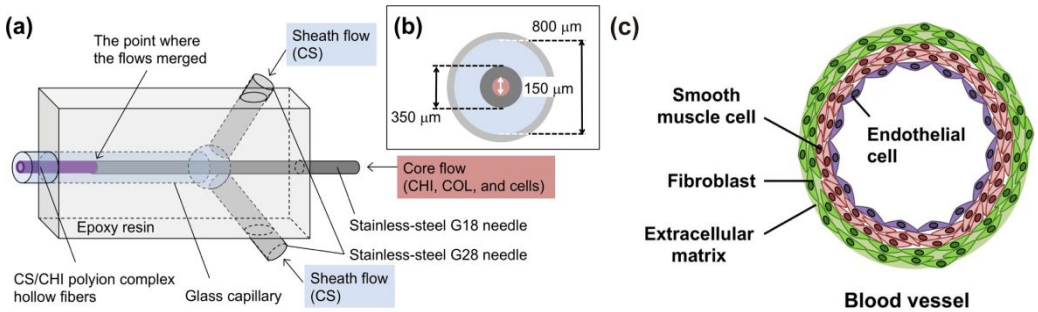

Fig 8 Microfluidics device and polysaccharides used in this study. (a) Schematic illustration of the microfluidic device and preparation of fibers, (b) sectioned illustration of the flow exit, and (c) artificial blood vessels. Reproduced with permission form ref. 158. Copyright 2019 American Chemical Society.

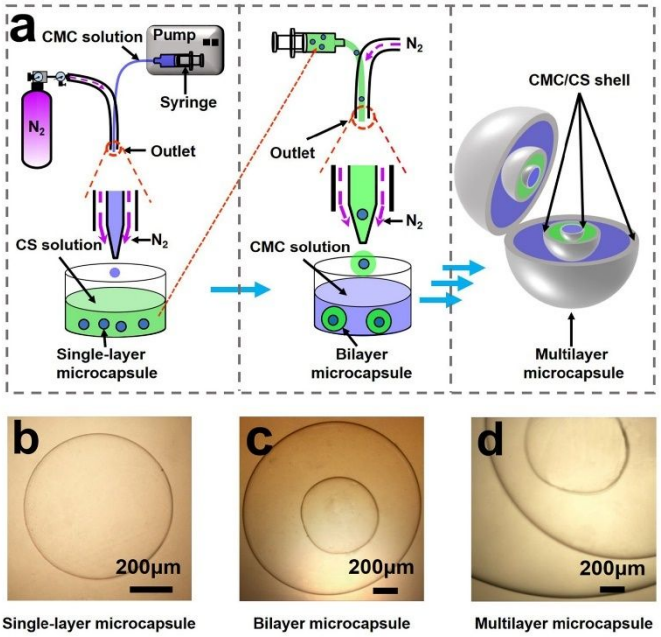

Fig 9 (a) Schematic illustration of the fabrication of LbL-assembled CMS/CS capsules by the gas-liquid microfluidic approach. Optical micrographs of CMC/CS single-layer capsule (b), CMC/CS bilayer capsule (c), and CMC/CS multilayer capsule (d). Reproduced with permission from ref. 161. Copyright 2017 Elsevier B. V.

3D bioprinting is a layer-by-layer fabrication approach in which cells and materials are processed together into a stratified three-dimensional order using an automated fabrication method.[166] While the variety of fabrication processes and applicable technologies have evolved in the last decade, the most commonly applied technologies are robotic dispensing, inkjet printing, and laser-assisted printing. Within the scope of this overview article, we want to focus on inkjet printing and laser-assisted printing as examples of bioprinting approaches.[167]

6.1. Inkjet printing

Inkjet printing, also known as drop-on-demand printing, is the most commonly used printing method for biomedical applications. Liquid printed from a nozzle is ejected into droplets with regulated volumes by thermal[168] or acoustic[28,169,170] (created by piezoelectric crystal) forces, then delivered to predetermined positions to form the final construct (**Fig 10a**). Inkjet printing as a layer-by-layer method offers advantages including high speed, precise controllability, low cost, and compatibility with many biomaterials.[31] Droplet size can be electronically controlled and the rate can reach up to 10,000 droplets per second.[28] The common drawback of inkjet printing is that the "ink" here refers to all of the biological materials that must be in a solution state for droplets to form. As a result, when printing cells, low cell concentrations are required to allow droplet formation and prevent nozzle clogging, making high cell densities difficult to obtain.

Inkjet printing combined with layer-by-layer technology enables the fabrication of complex structures that would be difficult to engineer using other methods. Suntivich[171] constructed silk fibrin nests consisting of up to 400 dots with diameters of 70-100 μm and thicknesses of 100-600 μm, printed a solution of E.coli at the center of each dot and then capped them with silk. This example demonstrates how inkjet printing is capable of constructing 3D structures with both chemical materials and living cells.

Bioprinting enables the fabrication of 3D-tissue architectures using the bottom-up principle, literally stacking cells layer-by-layer to match the natural structure. The biomaterial multilayers function as the ECM for nutrition and metabolic waste transfer. Layer-by-layer assembly between cells and biomaterials has been reported since 1998[172] when cells were inkjet printed on a thin collagen gel, then another thin layer of collagen was cast on top of the cells, and the procedure was repeated to generate cell/collagen multilayers. Dunn[173] sandwiched rat hepatocytes between two layers of hydrated rat tail tendon collagen matrix and found that the sandwiched hepatocytes sustained function better than those cultivated on a single layer of collagen. LbL films can also be used as a layer in cell/polymer multilayers, with the inkjet printed FN/collagen LbL films alternating with inkjet-printed cell layers. 3D tissue chips consisting of 440 micro-arrays with different layer numbers and cell types have been fabricated.[174]

Like polymeric LbL films, the properties of biological constructs can be adjusted by selecting different types of cell layers or alternating concentrations of the same cell,[175] allowing researchers to more accurately replicate the hierarchical architecture of real tissues and organs.[29] For instance, to obtain a 3D tissue structure with high liver functions, hepatocytes and endothelial cells, the two most abundant cell types in the liver, were used as "inks".[174] Various vascular cell types, including smooth muscle cell and fibroblast, were printed layer-by-layer concurrently with agarose rods as mold templates, resulting in single- and double-layered small vascular tubes with varying diameters.[176] The layer-by-layer printing of amniotic fluid-derived stem (AFS) cells into an alginate/collagen composite gel enable them to differentiate for specific functions.[68]

6.2. Laser-assisted bioprinting

Usually when printing cell layers, cells are suspended in an aqueous culture medium. The exposure of cells to heat and shear pressure at the nozzle tip may reduce cell viability so a new non-contact laser-assisted bioprinting technology has been developed.

Laser-assisted bioprinting (LAB), also known as matrix-assisted pulsed laser evaporation direct-write, is based on the principles of laser-induced forward transfer. It has been shown

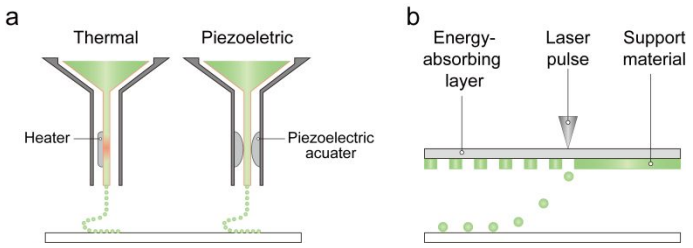

Fig 10 Scheme of 3D printing: (a) Inkjet printing and (b) laser-assisted printing.

to be capable of printing a variety of biological materials with high accuracy, including proteins, bacteria, and cells.[30,177,178] A typical LAB device consists of a pulsed laser beam, a focusing system, and a "ribbon" that is made from glass covered with a laser-energy-absorbing layer (gold or titanium) and a layer of biological materials.[32] As shown in **Fig 10b**, focused laser pulses on the absorbing layer generate high-pressure bubbles that cause the directional ejection of biomaterials from the support material to the substrate.[167] Because there is no nozzle in the LAB system, the problem of clogging with cells or high viscosity solutions that plague inkjet printing is not a factor. As such, this technology allows the printing of biomaterials with a wide range of viscosities and cell densities up to 10^8 cells/ml.[69] Moreover, the nozzle-free structure protects cells from shear pressure, which will not affect the viability and function of cell.

Due to its rapidity, precision, and ability to print living cells, this non-contact printing technology has been increasingly used in biomedical applications. For the first time in 2012, Koch[179] used LAB technology to deposit cells layer-by-layer to mimic tissue structures and functions. Fibroblasts and keratinocytes were embedded in collagen for the engineering of skin tissue with LbL assembly. As shown in **Fig 11**, the red and green layers (keratinocytes and fibroblasts, respectively) are distinct and do not overlap. One year later, Michael[177] increased the keratinocyte and fibroblast layers to 20 and transplanted the 3D cell construct to full-thickness skin wounds in mice. After 11 days of culture, the transplants were fully integrated into the surrounding tissue.

The construction of 3D tissues with improved functionality always needs more than one type of material. However, the addition of one component requires the preparation of an individual ribbon, which is time-consuming. If multiple cell types and materials are needed, the preparation work prior to

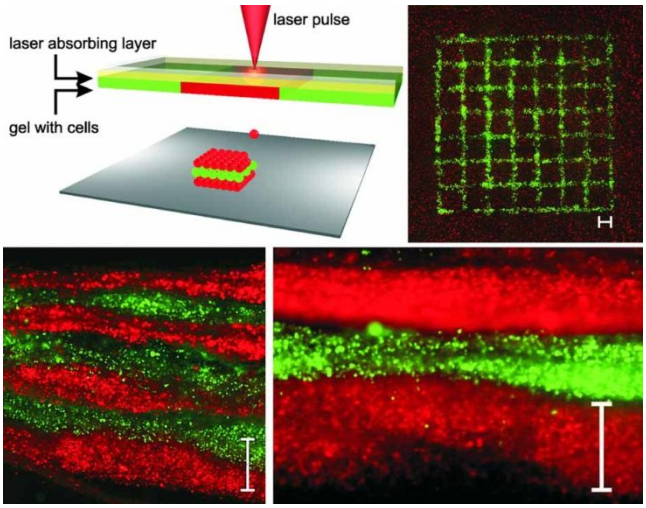

Fig 11 Sketch of the laser printing setup. The cell-hydrogel compound is propelled forward as a jet by the pressure of a laser-induced vapor bubble. Layer-by-layer a 3D cell pattern is generated. A printed grid structure (top view) of fibroblasts (green) and keratinocytes (red). The whole structure has a height of about 2 mm and a base area of 10 mm × 10 mm. scale bars are 500 µm. Reproduced with permission from ref. 191. Copyright 2012 WILEY-VCH.

printing can be particularly onerous. Besides, the biomaterials on the ribbon cannot be fully used and are hard to recycle, causing some waste which is a problem when the materials are rare and expensive. Overall, the high resolution of LAB and the ability to print high cell densities still makes it a competitive method for the rapid and accurate construction of 3D biomimetic materials.

3D printing is the most complicated LbL fabrication method. Because of its flexibility in shape-designing and "ink" selection, 3D printing LbL is almost used in tissue engineering. By mimicking the structure and composition of the real tissue, 3D printing is theoretically able to construct all kinds of tissues.

7. Challenges and perspectives

Over the past several decades, layer-by-layer assembly has experienced explosive development in methodologies and applications. The multitude of multilayer assembly technologies and their benefits in the construction of biomaterials have contributed to the growth of LbL assembly over a wide range of biomedical applications. The vast toolbox of LbL methodologies provides different options for the construction of desired structures.

Despite these advantages, LbL assembly for fabricating biomedical materials still faces some challenges. For macroscopic LbL assembly processes like dip, spin, and spray assembly, reducing material waste during the coating process remains important, especially for valuable materials such as some proteins and custom-synthesized polymers. For in vivo biological applications, the importance of material safety cannot be overstated.

Different LbL assembly methods possess their advantages and disadvantages. Most of the technical obstacles can be bypassed by selecting proper fabrication methods. However, one thing that cannot be avoided is the repeated deposition operation, even when using the fast spin and spray-assisted assembly method, we have to spin and spray multiple times to obtain thick films. The trade-off between film thickness and fabrication time needs to be considered during fabrication. LbL assembly on fragile substrates like cells. The mechanical forces by spin coating and high-pressure flow produced by spray and 3D printing nozzles may affect the viability of cells. But the time-consuming self-assembly technique requires cells to be in a non-culturable state for a longer period, which may lead to cell inactivation.

Since the LbL assembly technique has been studied for so long. Most LbL assembly needs two kinds of materials for interactions between the polymer chains. In most cases, however, the interactions occur between the side residues instead of the entire chains. In these cases, interactive domains, rather than having two different polymers, are necessary for LbL assembly. Assembly between single components helps us to study the effects of the chemical characteristics of that component on film properties. When considering in vivo application in particular, the interactions between tissues and materials can be very complicated so single-component assemblies are better for clarifying the underlying mechanism.

For polyelectrolytes, same-component LbL assembly does not rely on electrostatic interactions, making it possible for any polyelectrolytes to assemble, even those with the same charges. Early in 2006, Caruso's group[180] published the first paper on LbL multilayer assembly, essentially from the same polyelectrolytes. His group synthesized alkyne and azide modified polyacrylic acid (PAA), and the LbL was performed via click reaction. Single component LbL has since attracted the interest of researchers who have continued to enhance our understanding of single-component LbL. To date, a number of polyelectrolytes[181–183] have been used for single-component LbL, and the mechanism is not limited to click interactions between two same polymer backbones. Assemble with sacrificial layers[184–186] and small molecule mediated LbL assembly[187–190] are the other two methods widely used for single-component LbL assembly. Despite the differences in operation and mechanism, all the methods eventually yield multilayer films with organized structures composed of the same polymer backbone.

The development of LbL assembly methods is closely related to their integration with other technologies. Spin coating, spray coating, microfluidics, and 3D printing were not originally designed for LbL but their integration has increased the opportunities for LbL to be used in a range of biomedical applications. Because of the simplicity and great controllability of the assembled films, as well as the ability to combine with other technologies, LbL will continue to contribute to biomedical applications.

Conflicts of interest

There are no conflicts to declare.

Acknowledgements

This work was supported by JST SPRING, Grant Number JPMJSP2138, Grant-in-Aid for Scientific Research (A) (20H00665) from JSPS, Bilateral Programs between JSPS and DAAD (JPJSBP 120213505), Innovation Bridge Grant from Osaka University, and Grant-in-Aid for JSPS Research Fellow 202112833.

Notes and references

1 J. B. M. Rocha Neto, G. G. Lima, A. Fiamingo, L. G. L. Germiniani, T. B. Taketa, R. A. Bataglioli, G. A. T. da Silveira, J. V. L. da Silva, S. P. Campana-Filho, O. N. Oliveira and M. M. Beppu, *Int. J. Biol. Macromol.*, 2021, **172**, 154–161.

2 W.-H. Chen, G.-F. Luo, W.-X. Qiu, Q. Lei, L.-H. Liu, S.-B. Wang and X.-Z. Zhang, *Biomaterials*, 2017, **117**, 54–65.

3 J. Zheng, N. Rahman, L. Li, J. Zhang, H. Tan, Y. Xue, Y. Zhao, J. Zhai, N. Zhao, F. Xu, L. Zhang, R. Shi, Y. Lvov and J. Xue, *Mater. Sci. Eng. C*, 2021, **128**, 112295.

4 R. K. Iler, *J. Colloid Interface Sci.*, 1966, **21**, 569–594.

5 J. J. Kirkland, *Anal. Chem.*, 1965, **37**, 1458–1461.

6 G. Decher, *Science*, 1997, **277**, 1232–1237.

7 C. Zhou, J. Zhou, X. Ma, D. Pranantyo, J. Li, L. Xu and V. X. Truong, *Mater. Sci. Eng. C*, 2021, **121**, 111828.

8 A. vander Straeten, D. Lefèvre, S. Demoustier-Champagne and C. Dupont-Gillain, *Adv. Colloid Interface Sci.*, 2020, **280**, 102161.

9 A. L. Becker, A. P. R. Johnston and F. Caruso, *Macromol. Biosci.*, 2010, **10**, 488–495.

10 D. Kim, S. Cheong, Y. G. Ahn, S. W. Ryu, J.-K. Kim and J. Cho, *Nanoscale*, 2016, **8**, 7000–7016.

11 Y. Min and P. T. Hammond, *Chem. Mater.*, 2011, **23**, 5349–5357.

12 V. Selin, J. F. Ankner and S. A. Sukhishvili, *Macromolecules*, 2015, **48**, 3983–3990.

13 H. E. Karahan, L. Eyüboğlu, D. Kıyılar and A. L. Demirel, *Eur. Polym. J.*, 2014, **56**, 159–167.

14 E. Guzmán, H. Ritacco, F. Ortega and R. G. Rubio, *Colloids Surf. Physicochem. Eng. Asp.*, 2011, **384**, 274–281.

15 F. Croisier, G. Atanasova, Y. Poumay and C. Jérôme, *Adv. Healthc. Mater.*, 2014, **3**, 2032–2039.

16 J. J. Richardson, M. Björnmalm and F. Caruso, *Science*, 2015, **348**, aaa2491.

17 A. Zhuk, V. Selin, I. Zhuk, B. Belov, J. F. Ankner and S. A. Sukhishvili, *Langmuir*, 2015, **31**, 3889–3896.

18 A. C. Almeida, A. C. Vale, R. A. Pires, R. L. Reis and N. M. Alves, *J. Biomed. Mater. Res. B Appl. Biomater.*, 2020, **108**, 1412–1427.

19 S. Markutsya, C. Jiang, Y. Pikus and V. V. Tsukruk, *Adv. Funct. Mater.*, 2005, **15**, 771–780.

20 H. F. Alotaibi, Y. Al Thaher, S. Perni and P. Prokopovich, *Curr. Opin. Colloid Interface Sci.*, 2018, **36**, 130–142.

21 P. Schaaf, J.-C. Voegel, L. Jierry and F. Boulmedais, *Adv. Mater.*, 2012, **24**, 1001–1016.

22 S. W. Morton, K. P. Herlihy, K. E. Shopsowitz, Z. J. Deng, K. S. Chu, C. J. Bowerman, J. M. DeSimone and P. T. Hammond, *Adv. Mater.*, 2013, **25**, 4707–4713.

23 M. Michel, V. Toniazzo, D. Ruch and V. Ball, *ISRN Mater. Sci.*, 2012, **2012**, e701695.

24 K. Eawsakul, S. Tancharoen and N. Nasongkla, *J. Drug Deliv. Sci. Technol.*, 2021, **61**, 102296.

25 A. K. Miri, D. Nieto, L. Iglesias, H. Goodarzi Hosseinabadi, S. Maharjan, G. U. Ruiz-Esparza, P. Khoshakhlagh, A. Manbachi, M. R. Dokmeci, S. Chen, S. R. Shin, Y. S. Zhang and A. Khademhosseini, *Adv. Mater.*, 2018, **30**, 1800242.

26 H.-J. Kim, K. Lee, S. Kumar and J. Kim, *Langmuir*, 2005, **21**, 8532–8538.

27 A. S. Hansen, N. Hao and E. K. O'Shea, *Nat. Protoc.*, 2015, **10**, 1181–1197.

28 U. Demirci and G. Montesano, *Lab. Chip*, 2007, **7**, 1139–1145.

29 A. Lee, A. R. Hudson, D. J. Shiwarski, J. W. Tashman, T. J. Hinton, S. Yerneni, J. M. Bliley, P. G. Campbell and A. W. Feinberg, *Science*, 2019, **365**, 482–487.

30 O. Kérourédan, E. J. Ribot, J.-C. Fricain, R. Devillard and S. Miraux, *Sci. Rep.*, 2018, **8**, 15777.

31 P. Gao, A. Hunter, S. Benavides, M. J. Summe, F. Gao and W. A. Phillip, *ACS Appl. Mater. Interfaces*, 2016, **8**, 3386–3395.

32 J. A. Barron, B. R. Ringeisen, H. Kim, B. J. Spargo and D. B. Chrisey, *Thin Solid Films*, 2004, **453–454**, 383–387.

33 M. Criado-Gonzalez, C. Mijangos and R. Hernández, *Polymers*, 2021, **13**, 2254.

34 E. Kharlampieva, V. Kozlovskaya and S. A. Sukhishvili, *Adv. Mater.*, 2009, **21**, 3053–3065.

35 J. J. Richardson, J. Cui, M. Björnmalm, J. A. Braunger, H. Ejima and F. Caruso, *Chem. Rev.*, 2016, **116**, 14828–14867.

36 W. Tong, X. Song and C. Gao, *Chem. Soc. Rev.*, 2012, **41**, 6103–6124.

37 H. Sun, D. Choi, J. Heo, S. Y. Jung and J. Hong, *Cancers*, 2020, **12**, 593.

38 A. Sarode, A. Annapragada, J. Guo and S. Mitragotri, *Biomaterials*, 2020, **242**, 119929.

39 H. Ao, S. Yang, B. Nie, Q. Fan, Q. Zhang, J. Zong, S. Guo, X. Zheng and T. Tang, *J. Mater. Chem. B*, 2019, **7**, 1951–1961.

40 R. Kurapati, T. W. Groth and A. M. Raichur, *ACS Appl. Bio Mater.*, 2019, **2**, 5512–5527.

41 S. Guo, X. Zhu and X. J. Loh, *Mater. Sci. Eng. C*, 2017, **70**, 1163–1175.

42 J. Zeng, C. R. Correia, J. F. Mano and M. Matsusaki, *Biomacromolecules*, 2020, **21**, 4923–4932.

43 J. Zeng, N. Sasaki, C. R. Correia, J. F. Mano and M. Matsusaki, *Small*, 2020, **16**, 1907434.

44 J. L. Lutkenhaus, K. McEnnis and P. T. Hammond, *Macromolecules*, 2008, **41**, 6047–6054.

45 N. E. Muzzio, M. A. Pasquale, D. Gregurec, E. Diamanti, M. Kosutic, O. Azzaroni and S. E. Moya, *Macromol. Biosci.*, 2016, **16**, 482–495.

46 I. Zhuk, F. Jariwala, A. B. Attygalle, Y. Wu, M. R. Libera and S. A. Sukhishvili, *ACS Nano*, 2014, **8**, 7733–7745.

47 T. Fujie, M. Kinoshita, S. Shono, A. Saito, Y. Okamura, D. Saitoh and S. Takeoka, *Surgery*, 2010, **148**, 48–58.

48 T. Fujie, Y. Okamura and S. Takeoka, *Adv. Mater.*, 2007, **19**, 3549–3553.

49 J. Huang, X. Qiu, B. Yan, L. Xie, J. Yang, H. Xu, Y. Deng, L. Chen, X. Wang and H. Zeng, *J. Mater. Chem. B*, 2018, **6**, 3742–3750.

50 G. Cado, H. Kerdjoudj, A. Chassepot, M. Lefort, K. Benmlih, J. Hemmerlé, J.-C. Voegel, L. Jierry, P. Schaaf, Y. Frère and F. Boulmedais, *Langmuir*, 2012, **28**, 8470–8478.

51 K. C. Krogman, J. L. Lowery, N. S. Zacharia, G. C. Rutledge and P. T. Hammond, *Nat. Mater.*, 2009, **8**, 512–518.

52 M. Lefort, G. Popa, E. Seyrek, R. Szamocki, O. Felix, J. Hemmerlé, L. Vidal, J.-C. Voegel, F. Boulmedais, G. Decher and P. Schaaf, *Angew. Chem. Int. Ed.*, 2010, **49**, 10110–10113.

53 I. P. Monteiro, A. Shukla, A. P. Marques, R. L. Reis and P. T. Hammond, *J. Biomed. Mater. Res. A*, 2015, **103**, 330–340.

54 A. Shukla, J. C. Fang, S. Puranam, F. R. Jensen and P. T. Hammond, *Adv. Mater.*, 2012, **24**, 492–496.

55 D. Chen, Z. Kang, H. Hirahara and W. Li, *Appl. Surf. Sci.*, 2019, **481**, 1213–1219.

56 A. Shukla, S. N. Avadhany, J. C. Fang and P. T. Hammond, *Small*, 2010, **6**, 2392–2404.

57 A. Shukla, R. C. Fuller and P. T. Hammond, *J. Controlled Release*, 2011, **155**, 159–166.

58 J. T. O'Neal, M. J. Bolen, E. Y. Dai and J. L. Lutkenhaus, *J. Colloid Interface Sci.*, 2017, **485**, 260–268.

59 T. Masuda, M. Ukiki, Y. Yamagishi, M. Matsusaki, M. Akashi, U. Yokoyama and F. Arai, *J. Biotechnol.*, 2018, **276–277**, 46–53.

60 H.-J. Kim, K. Lee, S. Kumar and J. Kim, *Langmuir*, 2005, **21**, 8532–8538.

61 J. Fukuda, A. Khademhosseini, J. Yeh, G. Eng, J. Cheng, O. C. Farokhzad and R. Langer, *Biomaterials*, 2006, **27**, 1479–1486.

62 J. Son, C. Y. Bae and J.-K. Park, *JoVE J. Vis. Exp.*, 2016, e53475.

63 D. R. Reyes, E. M. Perruccio, S. P. Becerra, L. E. Locascio and M. Gaitan, *Langmuir*, 2004, **20**, 8805–8811.

64 J. Cui, H. Wang, Q. Shi, P. Ferraro, T. Sun, P. Dario, Q. Huang and T. Fukuda, *Acta Biomater.*, 2020, **113**, 328–338.

65 T. Liu, Y. Yin, Y. Yang, T. P. Russell and S. Shi, *Adv. Mater.*, 2022, **34**, 2105386.

66 D. Yu, L. Tang, Z. Dong, K. A. Loftis, Z. Ding, J. Cheng, B. Qin, J. Yan and W. Li, *Biomater. Sci.*, 2018, **6**, 2871–2880.

67 A. L. Yost, S. Shahsavari, G. M. Bradwell, R. Polak, F. Fachin, R. E. Cohen, G. H. McKinley, M. Toner, M. F. Rubner and B. L. Wardle, *Microsyst. Nanoeng.*, 2015, **1**, 1–7.

68 P. De Coppi, G. Bartsch, M. M. Siddiqui, T. Xu, C. C. Santos, L. Perin, G. Mostoslavsky, A. C. Serre, E. Y. Snyder, J. J. Yoo, M. E. Furth, S. Soker and A. Atala, *Nat. Biotechnol.*, 2007, **25**, 100–106.

69 B. Guillotin, A. Souquet, S. Catros, M. Duocastella, B. Pippenger, S. Bellance, R. Bareille, M. Rémy, L. Bordenave, J. Amédée and F. Guillemot, *Biomaterials*, 2010, **31**, 7250–7256.

70 S. Amorim, I. Pashkuleva, C. A. Reis, R. L. Reis and R. A. Pires, *J. Mater. Chem. B*, 2020, **8**, 3880–3885.

71 S. J. Gates and A. Shukla, *J. Polym. Sci. Part B Polym. Phys.*, 2017, **55**, 127–131.

72 V. Panchagnula, J. Jeon and A. V. Dobrynin, *Phys. Rev. Lett.*, 2004, **93**, 037801.

73 J. Zeng and M. Matsusaki, *Polym. Chem.*, 2019, **10**, 2960–2974.

74 M. P. Sousa, I. Gonzalez de Torre, M. B. Oliveira, J. C. Rodríguez-Cabello and J. F. Mano, *Mater. Today Chem.*, 2017, **4**, 150–163.

75 M. Guillot-Ferriols, A. del Barrio, C. M. Costa, S. Lanceros Méndez, J. C. Rodríguez-Cabello, J. L. Gómez Ribelles, M. Santos and G. Gallego Ferrer, *Eur. Polym. J.*, 2021, **146**, 110269.

76 H. Yan, X. Chen, M. Feng, Z. Shi, D. Zhang and Q. Lin, *Mater. Lett.*, 2017, **209**, 492–496.

77 T.-D. Zhang, X. Deng, Y.-F. Wang, X.-T. Wang, X. Zhang, L.-L. Chen, X. Cao, Y.-Z. Zhang, C.-Y. Zhang, X. Zheng and D.-C. Yin, *Appl. Surf. Sci.*, 2020, **530**, 147197.

78 X. Wang, R. Wang, F. Wu, H. Yue, Z. Cui, X. Zhou and Y. Lu, *Eur. Polym. J.*, 2021, **158**, 110689.

79 M. Kitsara, G. Tassis, A. Papagiannopoulos, A. Simon, O. Agbulut and S. Pispas, *Macromol. Biosci.*, 2022, **22**, 2100346.

80 T. Crouzier, K. Ren, C. Nicolas, C. Roy and C. Picart, *Small*, 2009, **5**, 598–608.

81 S. Guo, X. Zhu, M. Li, L. Shi, J. L. T. Ong, D. Jańczewski and K. G. Neoh, *ACS Appl. Mater. Interfaces*, 2016, **8**, 30552–30563.

82 D. Yılmaz Aykut, Ö. Yolaçan and H. Deligöz, *Colloids Surf. Physicochem. Eng. Asp.*, 2020, **602**, 125113.

83 Y. Qu, T. Wei, W. Zhan, C. Hu, L. Cao, Q. Yu and H. Chen, *J. Mater. Chem. B*, 2017, **5**, 444–453.

84 F. Lv, L. Xu, Y. Zhang and Z. Meng, *ACS Appl. Mater. Interfaces*, 2015, **7**, 19104–19111.

85 T. He, D. Jańczewski, S. Guo, S. M. Man, S. Jiang and W. S. Tan, *Colloids Surf. B Biointerfaces*, 2018, **161**, 269–278.

86 J. Woo, Y. Na, W. I. Choi, S. Kim, J. Kim, J. Hong and D. Sung, *Acta Biomater.*, 2021, **125**, 242–252.

87 B. Zhang, R. Yao, C. Hu, M. F. Maitz, H. Wu, K. Liu, L. Yang, R. Luo and Y. Wang, *Biomaterials*, 2021, **269**, 120418.

88 Y. Wang, B. Ma, A. Yin, B. Zhang, R. Luo, J. Pan and Y. Wang, *J Control Release*, 2020, **320**, 226–238.

89 P. Gentile, A. M. Ferreira, J. T. Callaghan, C. A. Miller, J. Atkinson, C. Freeman and P. V. Hatton, *Adv. Healthc. Mater.*, 2017, **6**, 1601182.

90 T. Crouzier, F. Sailhan, P. Becquart, R. Guillot, D. Logeart-Avramoglou and C. Picart, *Biomaterials*, 2011, **32**, 7543–7554.

91 R. Guillot, I. Pignot-Paintrand, J. Lavaud, A. Decambron, E. Bourgeois, V. Josserand, D. Logeart-Avramoglou, E. Viguier and C. Picart, *Acta Biomater.*, 2016, **36**, 310–322.

92 R. Guillot, F. Gilde, P. Becquart, F. Sailhan, A. Lapeyrere, D. Logeart-Avramoglou and C. Picart, *Biomaterials*, 2013, **34**, 5737–5746.

93 Y. Yan, M. Björnmalm and F. Caruso, *Chem. Mater.*, 2014, **26**, 452–460.

94 E. Donath, G. B. Sukhorukov, F. Caruso, S. A. Davis and H. Möhwald, *Angew. Chem. Int. Ed.*, 1998, **37**, 2201–2205.

95 Y. Ni, D. Zhang, Y. Wang, X. He, J. He, H. Wu, J. Yuan, D. Sha, L. Che, J. Tan and J. Yang, *ACS Appl. Mater. Interfaces*, 2021, **13**, 14543–14551.

96 M. V. Lomova, A. I. Brichkina, M. V. Kiryukhin, E. N. Vasina, A. M. Pavlov, D. A. Gorin, G. B. Sukhorukov and M. N. Antipina, *ACS Appl. Mater. Interfaces*, 2015, **7**, 11732–11740.

97 H. Lin, W. Xiao, S.-Y. Qin, S.-X. Cheng and X.-Z. Zhang, *Polym. Chem.*, 2014, **5**, 4437–4440.

98 R. R. Costa, E. Castro, F. J. Arias, J. C. Rodríguez-Cabello and J. F. Mano, *Biomacromolecules*, 2013, **14**, 2403–2410.

99 C. R. Correia, R. P. Pirraco, M. T. Cerqueira, A. P. Marques, R. L. Reis and J. F. Mano, *Sci. Rep.*, 2016, **6**, 21883.

100D. Hong and S. H. Yang, *Macromol. Res.*, 2018, **26**, 1185–1192.

101M. B. Oliveira, J. Hatami and J. F. Mano, *Chem. – Asian J.*, 2016, **11**, 1753–1764.

102Y. Choi, B. Phan, M. Tanaka, J. Hong and J. Choi, *ACS Appl. Bio Mater.*, 2020, **3**, 6556–6570.

103T. Liu, Y. Wang, W. Zhong, B. Li, K. Mequanint, G. Luo and M. Xing, *Adv. Healthc. Mater.*, 2019, **8**, 1800939.

104C. R. Correia, S. Nadine and J. F. Mano, *Adv. Funct. Mater.*, 2020, **30**, 1908061.

105P. Gentile, I. Carmagnola, T. Nardo and V. Chiono, *Nanotechnology*, 2015, **26**, 422001.

106R. F. Fakhrullin, A. I. Zamaleeva, M. V. Morozov, D. I. Tazetdinova, F. K. Alimova, A. K. Hilmutdinov, R. I. Zhdanov, M. Kahraman and M. Culha, *Langmuir*, 2009, **25**, 4628–4634.

107A. I. Zamaleeva, I. R. Sharipova, A. V. Porfireva, G. A. Evtugyn and R. F. Fakhrullin, *Langmuir*, 2010, **26**, 2671–2679.

108R. F. Fakhrullin and Y. M. Lvov, *ACS Nano*, 2012, **6**, 4557–4564.

109J.-Z. Wang, Z.-Q. Ding, F. Zhang and W.-B. Ye, *Mater. Sci. Eng. C*, 2017, **77**, 1247–1260.

110B. J. Kim, H. Cho, J. H. Park, J. F. Mano and I. S. Choi, *Adv. Mater.*, 2018, **30**, 1706063.

111M. Matsusaki, K. Kadowaki, Y. Nakahara and M. Akashi, *Angew. Chem. Int. Ed.*, 2007, **46**, 4689–4692.

112A. Nishiguchi, H. Yoshida, M. Matsusaki and M. Akashi, *Adv. Mater.*, 2011, **23**, 3506–3510.

113P. Sher, C. A. Custódio and João. F. Mano, *Small*, 2010, **6**, 2644–2648.

114P. Sher, C. R. Correia, R. R. Costa and J. F. Mano, *RSC Adv.*, 2014, **5**, 2511–2516.

115J. M. Silva, A. R. C. Duarte, C. A. Custódio, P. Sher, A. I. Neto, A. C. M. Pinho, J. Fonseca, R. L. Reis and J. F. Mano, *Adv. Healthc. Mater.*, 2014, **3**, 433–440.

116P. A. Chiarelli, M. S. Johal, J. L. Casson, J. B. Roberts, J. M. Robinson and H.-L. Wang, *Adv. Mater.*, 2001, **13**, 1167–1171.

117J. Cho, K. Char, J.-D. Hong and K.-B. Lee, *Adv. Mater.*, 2001, **13**, 1076–1078.

118J. Hernandez-Montelongo, D. Gallach, N. Naveas, V. Torres-Costa, A. Climent-Font, J. P. García-Ruiz and M. Manso-Silvan, *Mater. Sci. Eng. C*, 2014, **34**, 245–251.

119Y. Xiang, J. Li, X. Liu, Z. Cui, X. Yang, K. W. K. Yeung, H. Pan and S. Wu, *Mater. Sci. Eng. C*, 2017, **79**, 629–637.

120K. Norrman, A. Ghanbari-Siahkali and N. B. Larsen, *Annu. Rep. Sect. C Phys. Chem.*, 2005, **101**, 174.

121P. J. Yoo, K. T. Nam, J. Qi, S.-K. Lee, J. Park, A. M. Belcher and P. T. Hammond, *Nat. Mater.*, 2006, **5**, 234–240.

122P. J. Yoo, N. S. Zacharia, J. Doh, K. T. Nam, A. M. Belcher and P. T. Hammond, *ACS Nano*, 2008, **2**, 561–571.

123L. Xu, J. F. Ankner and S. A. Sukhishvili, *Macromolecules*, 2011, **44**, 6518–6524.

124L. Xu, V. Kozlovskaya, E. Kharlampieva, J. F. Ankner and S. A. Sukhishvili, *ACS Macro Lett.*, 2012, **1**, 127–130.

125H. Zhang, D. Wang, Z. Wang and X. Zhang, *Eur. Polym. J.*, 2007, **43**, 2784–2791.

126W. Cai, J. Wu, C. Xi, A. J. Ashe and M. E. Meyerhoff, *Biomaterials*, 2011, **32**, 7774–7784.

127R. A. Ghostine, R. M. Jisr, A. Lehaf and J. B. Schlenoff, *Langmuir*, 2013, **29**, 11742–11750.

128S. Liu, Y. Cao, Z. Wu and H. Chen, *J. Mater. Chem. B*, 2020, **8**, 5529–5534.

129R. Yuan, C. Luo, Y. Yang, C. He, Z. Lu and L. Ge, *Adv. Mater. Interfaces*, 2020, **7**, 1901873.

130S. Williams, A. Wakisaka, Q. Q. Zeng, J. Barnes, G. Martin, W. J. Wechter and C. T. Liang, *Bone*, 1996, **19**, 637–644.

131X. Shen, H. Gu, P. Ma, Z. Luo, M. Li, Y. Hu and K. Cai, *Mater. Sci. Eng. C*, 2019, **102**, 696–707.

132H. Zhou, J. Li, J. Li, Q. Ruan, X. Peng, S. Li, W. Jin, Z. Yu, P. K. Chu and W. Li, *Surf. Coat. Technol.*, 2021, **412**, 127078.

133A. A. Mamedov and N. A. Kotov, *Langmuir*, 2000, **16**, 5530–5533.

134L. Shen, B. Wang, J. Wang, J. Fu, C. Picart and J. Ji, *ACS Appl. Mater. Interfaces*, 2012, **4**, 4476–4483.

135A. L. Larkin, R. M. Davis and P. Rajagopalan, *Biomacromolecules*, 2010, **11**, 2788–2796.

136S. G. Caridade, C. Monge, F. Gilde, T. Boudou, J. F. Mano and C. Picart, *Biomacromolecules*, 2013, **14**, 1653–1660.

137M. E. Nash, D. Healy, W. M. Carroll, C. Elvira and Y. A. Rochev, *J. Mater. Chem.*, 2012, **22**, 19376–19389.

138J. Yang, M. Yamato, C. Kohno, A. Nishimoto, H. Sekine, F. Fukai and T. Okano, *Biomaterials*, 2005, **26**, 6415–6422.

139A. D. Stroock, R. S. Kane, M. Weck, S. J. Metallo and G. M. Whitesides, *Langmuir*, 2003, **19**, 2466–2472.

140T. Fujie, A. Saito, M. Kinoshita, H. Miyazaki, S. Ohtsubo, D. Saitoh and S. Takeoka, *Biomaterials*, 2010, **31**, 6269–6278.

141Y. Okamura, K. Kabata, M. Kinoshita, D. Saitoh and S. Takeoka, *Adv. Mater.*, 2009, **21**, 4388–4392.

142A. Hinoki, A. Saito, M. Kinoshita, J. Yamamoto, D. Saitoh and S. Takeoka, *Br. J. Surg.*, 2016, **103**, 692–700.

143E. Redolfi Riva, A. Desii, E. Sinibaldi, G. Ciofani, V. Piazza, B. Mazzolai and V. Mattoli, *ACS Nano*, 2014, **8**, 5552–5563.

144J. B. Schlenoff, S. T. Dubas and T. Farhat, *Langmuir*, 2000, **16**, 9968–9969.

145A. Izquierdo, S. S. Ono, J.-C. Voegel, P. Schaaf and G. Decher, *Langmuir*, 2005, **21**, 7558–7567.

146T. C. Reis, S. Castleberry, A. M. B. Rego, A. Aguiar-Ricardo and P. T. Hammond, *Biomater. Sci.*, 2016, **4**, 319–330.

147M.-Q. Zhao, N. Trainor, C. E. Ren, M. Torelli, B. Anasori and Y. Gogotsi, *Adv. Mater. Technol.*, 2019, **4**, 1800639.

148M. Criado-Gonzalez, M. Fernandez-Gutierrez, J. San Roman, C. Mijangos and R. Hernández, *Carbohydr. Polym.*, 2019, **206**, 428–434.

149C. Nie, Y. Yang, C. Cheng, L. Ma, J. Deng, L. Wang and C. Zhao, *Acta Biomater.*, 2017, **51**, 479–494.

150Y. Wang, Y. Liu, Y. Cheng, E. Kim, G. W. Rubloff, W. E. Bentley and G. F. Payne, *Adv. Mater.*, 2011, **23**, 5817–5821.

151H. Katayama, Y. Ishihama and N. Asakawa, *Anal. Chem.*, 1998, **70**, 5272–5277.

152K. Kowsari, B. Zhang, S. Panjwani, Z. Chen, H. Hingorani, S. Akbari, N. X. Fang and Q. Ge, *Addit. Manuf.*, 2018, **24**, 627–638.

153C. Sun, N. Fang, D. M. Wu and X. Zhang, *Sens. Actuators Phys.*, 2005, **121**, 113–120.

154N. Raman, M.-R. Lee, S. P. Palecek and D. M. Lynn, *J. Controlled Release*, 2014, **191**, 54–62.

155S. Hong, S. S. Yoo, G. H. Choi, J. H. Lee, Y.-W. Choi, M. Kim, E. Kim, S. J. Kwon, D. J. Kim, J. Park and P. J. Yoo, *Compos. Part B Eng.*, 2022, **230**, 109537.

156Z. Wu, D. Zhao, C. Hou, L. Liu, J. Chen, H. Huang, Q. Zhang, Y. Duan, Y. Li and H. Wang, *Nanoscale*, 2018, **10**, 17663–17670.

157B. Aor, I. Khan, K. Glinel, A. M. Jonas, S. Demoustier-Champagne and M.-C. Durrieu, *ACS Appl. Bio Mater.*, 2020, **3**, 1520–1532.

158K. Iijima, S. Ichikawa, S. Ishikawa, D. Matsukuma, Y. Yataka, H. Otsuka and M. Hashizume, *ACS Biomater. Sci. Eng.*, 2019, **5**, 5688–5697.

159X. Li, N. R. Visaveliya, L. Hafermann, A. Knauer, S. Schneider and J. M. Köhler, *ACS Appl. Nano Mater.*, 2018, **1**, 6398–6406.

160E. Jeong, G. Lee, S. W. Han, W. J. Lee, H. S. Choi, Y. Lee and J. W. Kim, *J. Ind. Eng. Chem.*, 2017, **46**, 192–198.

161Y. Wang, J. Zhou, X. Guo, Q. Hu, C. Qin, H. Liu, M. Dong and Y. Chen, *Mater. Sci. Eng. C*, 2017, **81**, 13–19.

162H. Herrada-Manchón, L. Celada, D. Rodríguez-González, M. Alejandro Fernández, E. Aguilar and M.-D. Chiara, *Mater. Sci. Eng. C*, 2021, **128**, 112357.

163B. R. Ringeisen, C. M. Othon, J. A. Barron, D. Young and B. J. Spargo, *Biotechnol. J.*, 2006, **1**, 930–948.

164J. Alper, *Science*, 2004, **305**, 1895–1895.

165V. Mironov, R. P. Visconti, V. Kasyanov, G. Forgacs, C. J. Drake and R. R. Markwald, *Biomaterials*, 2009, **30**, 2164–2174.

166J. Groll, T. Boland, T. Blunk, J. A. Burdick, D.-W. Cho, P. D. Dalton, B. Derby, G. Forgacs, Q. Li, V. A. Mironov, L. Moroni, M. Nakamura, W. Shu, S. Takeuchi, G. Vozzi, T. B. F. Woodfield, T. Xu, J. J. Yoo and J. Malda, *Biofabrication*, 2016, **8**, 013001.

167S. V. Murphy and A. Atala, *Nat. Biotechnol.*, 2014, **32**, 773–785.

168X. Cui, T. Boland, D. D.D'Lima and M. K. Lotz, *Recent Pat. Drug Deliv. Formul.*, 2012, **6**, 149–155.

169R. E. Saunders, J. E. Gough and B. Derby, *Biomaterials*, 2008, **29**, 193–203.

170T. Xu, H. Kincaid, A. Atala and J. J. Yoo, *J. Manuf. Sci. Eng.*, 2008, **130**, 021017.

171R. Suntivich, I. Drachuk, R. Calabrese, D. L. Kaplan and V. V. Tsukruk, *Biomacromolecules*, 2014, **15**, 1428–1435.

172R. J. Klebe, *Exp. Cell Res.*, 1988, **179**, 362–373.

173J. C. Y. Dunn, R. G. Tompkins and M. L. Yarmush, *Biotechnol. Prog.*, 1991, **7**, 237–245.

174M. Matsusaki, K. Sakaue, K. Kadowaki and M. Akashi, *Adv. Healthc. Mater.*, 2013, **2**, 534–539.

175A. Dimaraki, P. J. Díaz-Payno, M. Minneboo, M. Nouri-Goushki, M. Hosseini, N. Kops, R. Narcisi, M. J. Mirzaali, G. J. V. M. van Osch, L. E. Fratila-Apachitei and A. A. Zadpoor, *Appl. Sci.*, 2021, **11**, 7821.

176C. Norotte, F. S. Marga, L. E. Niklason and G. Forgacs, *Biomaterials*, 2009, **30**, 5910–5917.

177S. Michael, H. Sorg, C.-T. Peck, L. Koch, A. Deiwick, B. Chichkov, P. M. Vogt and K. Reimers, *PLOS ONE*, 2013, **8**, e57741.

178J. A. Barron, P. Wu, H. D. Ladouceur and B. R. Ringeisen, *Biomed. Microdevices*, 2004, **6**, 139–147.

179L. Koch, A. Deiwick, S. Schlie, S. Michael, M. Gruene, V. Coger, D. Zychlinski, A. Schambach, K. Reimers, P. M. Vogt and B. Chichkov, *Biotechnol. Bioeng.*, 2012, **109**, 1855–1863.

180G. K. Such, J. F. Quinn, A. Quinn, E. Tjipto and F. Caruso, *J. Am. Chem. Soc.*, 2006, **128**, 9318–9319.

181C. J. Ochs, G. K. Such, B. Städler and F. Caruso, *Biomacromolecules*, 2008, **9**, 3389–3396.

182C. R. Kinnane, G. K. Such and F. Caruso, *Macromolecules*, 2011, **44**, 1194–1202.

183C. Lu, B. Mu and P. Liu, *Colloids Surf. B Biointerfaces*, 2011, **83**, 254–259.

184C. Liu, E. Thormann, P. M. Claesson and E. Tyrode, *Langmuir*, 2014, **30**, 8878–8888.

185Y. Lu, Y. Wu, J. Liang, M. R. Libera and S. A. Sukhishvili, *Biomaterials*, 2015, **45**, 64–71.

186X. Liang, V. Kozlovskaya, Y. Chen, O. Zavgorodnya and E. Kharlampieva, *Chem. Mater.*, 2012, **24**, 3707–3719.

187T. R. Sinclair, A. Patil, B. G. Raza, D. Reurink, S. K. van den Hengel, S. A. Rutjes, A. M. de Roda Husman, H. D. W. Roesink and W. M. de Vos, *J. Membr. Sci.*, 2019, **570–571**, 494–503.

188J. He, Y. Guan and Y. Zhang, *J. Appl. Polym. Sci.*, 2013, **129**, 3070–3076.

189F. Bucatariu, G. Fundueanu, G. Hitruc and E. S. Dragan, *Colloids Surf. Physicochem. Eng. Asp.*, 2011, **380**, 111–118.

190U. Manna, J. Dhar, R. Nayak and S. Patil, *Chem. Commun.*, 2010, **46**, 2250–2252.

191L. Koch, A. Deiwick, S. Schlie, S. Michael, M. Gruene, V. Coger, D. Zychlinski, A. Schambach, K. Reimers, P. M. Vogt and B. Chichkov, *Biotechnol. Bioeng.*, 2012, **109**, 1855–1863.